Cancer Research

Loss of Pax5 Exploits Sca1-BCR-ABL^{p190} Susceptibility to Confer the Metabolic Shift Essential for pB-ALL

Alberto Martín-Lorenzo[1,2], Franziska Auer[3,4], Lai N. Chan[3], Idoia García-Ramírez[1,2], Inés González-Herrero[1,2], Guillermo Rodríguez-Hernández[1,2], Christoph Bartenhagen[5], Martin Dugas[5], Michael Gombert[4], Sebastian Ginzel[4], Oscar Blanco[6], Alberto Orfao[7], Diego Alonso-López[8], Javier De Las Rivas[2,9], Maria B. García-Cenador[10], Francisco J. García-Criado[10], Markus Müschen[3], Isidro Sánchez-García[1,2], Arndt Borkhardt[5], Carolina Vicente-Dueñas[1,2], and Julia Hauer[5]

Downloaded from http://aacrjournals.org/cancerres/article-pdf/78/10/2669/2764846/2669.pdf by guest on 05 February 2024

Abstract

Preleukemic clones carrying *BCR-ABL^{p190}* oncogenic lesions are found in neonatal cord blood, where the majority of preleukemic carriers do not convert into precursor B-cell acute lymphoblastic leukemia (pB-ALL). However, the critical question of how these preleukemic cells transform into pB-ALL remains undefined. Here, we model a BCR-ABL^{p190} preleukemic state and show that limiting BCR-ABL^{p190} expression to hematopoietic stem/progenitor cells (HS/PC) in mice (Sca1-BCR-ABL^{p190}) causes pB-ALL at low penetrance, which resembles the human disease. pB-ALL blast cells were BCR-ABL–negative and transcriptionally similar to pro-B/pre-B cells, suggesting disease onset upon reduced Pax5 functionality. Consistent with this, double Sca1-BCR-ABL^{p190}+*Pax5*$^{+/-}$ mice developed pB-ALL with shorter latencies, 90% incidence, and accumulation of genomic alterations in the remaining wild-type *Pax5* allele. Mechanistically, the Pax5-deficient leukemic pro-B cells exhibited a metabolic switch toward increased glucose utilization and energy metabolism. Transcriptome analysis revealed that metabolic genes (*IDH1*, *G6PC3*, *GAPDH*, *PGK1*, *MYC*, *ENO1*, *ACO1*) were upregulated in Pax5-deficient leukemic cells, and a similar metabolic signature could be observed in human leukemia. Our studies unveil the first *in vivo* evidence that the combination between Sca1-BCR-ABL^{p190} and metabolic reprogramming imposed by reduced Pax5 expression is sufficient for pB-ALL development. These findings might help to prevent conversion of BCR-ABL^{p190} preleukemic cells.

Significance: Loss of Pax5 drives metabolic reprogramming, which together with Sca1-restricted BCR-ABL expression enables leukemic transformation. *Cancer Res; 78(10); 2669–79. ©2018 AACR.*

Introduction

Although preleukemic clones carrying BCR-ABL^{p190} oncogenic lesions are frequently found in neonatal cord blood (1, 2), they often remain silent, because the majority of these carriers do not develop precursor B-cell acute lymphoblastic leukemia (pB-ALL). In addition, small fractions of normal B cells in healthy adults carry silent BCR-ABL oncogenes (3). These findings suggest that BCR-ABL^{p190} might promote leukemogenesis by creating an aberrant progenitor compartment that is susceptible to malignant transformation through accumulation of additional secondary hits, which act as drivers of leukemogenesis. Thus, *BCR-ABL^{p190}* does not seem to be a dominant oncogene within the natural cellular hematopoietic stem/progenitor cell (HS/PC) compartment where the BCR-ABL^{p190} oncogenic lesion takes place. This is further supported by both clinical data showing that BCR-ABL^{p190}-induced tumorigenesis is not reversible through the unique inactivation of the gene defect initiating leukemia development (4), and by murine *in vivo* data showing that suppression of BCR-ABL^{p190} in leukemic mice carrying a tetracycline-repressible BCR-ABL^{p190} transgene did not rescue the malignant phenotype (5). However, the mode of action that BCR-ABL^{p190} exerts in the HS/PC compartment, remains difficult to demonstrate using available models of transgenic-driven BCR-ABL ALL

[1]Experimental Therapeutics and Translational Oncology Program, Instituto de Biología Molecular y Celular del Cáncer, CSIC/Universidad de Salamanca, Campus M. de Unamuno s/n, Salamanca, Spain. [2]Institute of Biomedical Research of Salamanca (IBSAL), Salamanca, Spain. [3]Department of Systems Biology, Beckman Research Institute, Monrovia, California. [4]Department of Pediatric Oncology, Hematology and Clinical Immunology, Heinrich-Heine University Dusseldorf, Medical Faculty, Dusseldorf, Germany. [5]Institute of Medical Informatics, University of Muenster, Muenster, Germany. [6]Departamento de Anatomía Patológica, Universidad de Salamanca, Salamanca, Spain. [7]Servicio de Citometría and Departamento de Medicina, Universidad de Salamanca, Salamanca, Spain. [8]Bioinformatics Unit, Cancer Research Center (CSIC-USAL) Salamanca, Spain. [9]Bioinformatics and Functional Genomics Research Group, Cancer Research Center (CSIC-USAL), Salamanca, Spain. [10]Departamento de Cirugía, Universidad de Salamanca, Salamanca, Spain.

Note: Supplementary data for this article are available at Cancer Research Online (http://cancerres.aacrjournals.org/).

Corrected online July 19, 2018.

A. Martín-Lorenzo, F. Auer, and L.N. Chan are co-first authors of this article.

Corresponding Author: Julia Hauer, Heinrich-Heine University Dusseldorf, Moorenstr. 5, Duesseldorf 40225, Germany. Phone: 4902-1181-17680; Fax: 4902-1181-16707; E-mail: Julia.Hauer@med.uni-duesseldorf.de; M. Müschen, E-mail: muschen@coh.org; I. Sánchez-García, isg@usal.es; A. Borkhardt, E-mail: Arndt.Borkhardt@med.uni-duesseldorf.de; and C. Vicente-Dueñas, E-mail: cvd@usal.es

doi: 10.1158/0008-5472.CAN-17-3262

©2018 American Association for Cancer Research.

(6, 7), because the penetrance of most of the respective pB-ALL disease models is 100%. Thus, current available models are not able to mimic the human scenario, where the presence of the BCR-ABL transgene in HS/PCs does not necessarily lead to disease development, but mainly generates a susceptibility that is preserved in the cancer-initiating cells. In this work, we explored a novel mode of action of BCR-ABL^{P190} in HS/PCs, utilizing mice with restricted expression of the *BCR-ABL^{p190}* oncogene to the stem/progenitor cell compartment.

Materials and Methods

Generation of Sca1-BCR-ABL^{P190} and Sca1-BCR-ABL^{P190}+Pax5$^{+/-}$

The heterozygous *Pax5*$^{+/-}$ mice (8) have been described previously. Heterozygous *Pax5*$^{+/-}$ mice were bred to Sca1-TK-IRES-BCR-ABL^{P190} mice to generate compound heterozygotes. The Sca1-TK-IRES-BCR-ABL^{P190} vector was generated as follows. The 9 kb EcoRI-EcoRI TK-IRES-BCR-ABL^{P190} cassette was inserted into the ClaI site of the pLy6 vector (9), resulting in Sca1-TK-IRES-BCR-ABL^{P190} vector. The transgene fragment was excised from its vector by restriction digestion with NotI, purified for injection (2 ng/mL) and injected into CBAxC57BL/6J fertilized eggs. Transgenic mice were identified by Southern analysis of tail snip DNA after *Eco*RI digestion. Human *ABL* cDNA was used for detection of the transgene. Two founder lines were obtained for the *Sca1-BCR-ABL^{p190}* transgene with different positional integration of the transgenic construct in both lines. All animal work has been conducted according to relevant national and international guidelines and it has been approved by the Bioethics Committee of University of Salamanca and by the Bioethics Subcommittee of Consejo Superior de Investigaciones Cientificas (CSIC). For all genotypes both male and female mice of a mixed C57BL/6 × CBA background were included in the study. We systematically used littermates of the same breeding. Upon signs of disease, mice were sacrificed and subjected to standard necropsy procedures. All major organs were examined under the dissecting microscope. Tissue samples were taken from homogenous portions of the resected organ and fixed immediately after excision. Differences in Kaplan–Meier survival plots of transgenic and WT mice were analyzed using the log-rank (Mantel–Cox) test.

Real-time analysis (BCR-ABL^{P190})

cDNA used in qPCR studies was synthesized using reverse transcriptase (Access RT-PCR System; Promega). Two microliters of second round amplified RNA was transcribed. Primers and probes used for quantitative PCR have been described previously (10). The probes were designed so that genomic DNA would not be detected during the PCR. The sequences of the specific primers and probes were as follows: BCR-ABL^{P190}, sense primer 5′-CCGCAAGACCGGGCAGAT-3′, antisense primer 5′-CAGATGCTACTGGCCGCTGA-3′ and probe 5′-TGGCCCAACGATGGCGAGGG-3′; c-Abl, sense primer 5′-CACTCTCAGCATCACTAAAGGTGAA-3′, antisense primer 5′-CGTTTGGGCTTCACACCATT-3′, and probe 5′-CCGGGTCTTGGGTTATAATCACAATG-3′.

qRT-PCR of *Hk2, Ldha Slc2a3, Idh1,* and *Pgk1*

We analyzed expression of Hk2, Ldha, Slc2a3, Idh1, and Pgk1 in both leukemic BCR-ABL^{P190} and leukemic BCR-ABL^{P190}+Pax5$^{+/-}$ cells by qRT-PCR as follows: cDNA was synthesized using reverse transcriptase (Access RT-PCR System; Promega) and genomic DNA was removed by DNAase treatment (Roche, 04 716 728 001). Real-time PCR reactions were performed in an Eppendorf MasterCycler Realplex machine.

Commercially available assays for quantitative PCR from IDT (Integrated DNA Technologies) were used: Hk2 (Assay ID: Mm.PT.S832698746), Ldha (Assay ID: Mm.PT.58.29860774), Slc2a3 (Assay ID: Mm.PT.30464830), Idh1 (Assay ID: Mm.PT.58.5996441), Pgk1 (Assay ID: Mm.PT.39a.22214854), and RplpO (Assay ID: Mm.PT.58.43894205). Probes were specifically designed to prevent detection of genomic DNA by PCR. Measurement of RplpO gene product expression was used as an endogenous control. All samples were run in triplicate. The comparative CT Method (ΔΔCt) was used to calculate relative expression of the transcript of interest and a positive control.

Microarray data and enrichment analysis

Total RNA was isolated in two steps using Trizol (Life Technologies), followed by RNeasy Mini Kit (Qiagen) purification following the manufacturer's RNA Clean-up protocol with the optional On-column DNase treatment. Integrity and quality of the RNA were verified by electrophoresis. Samples were analyzed using Affymetrix Mouse Gene 1.0 ST Arrays.

The data discussed in this publication have been deposited in NCBI's Gene Expression Omnibus (11) and are accessible through GEO Series accession number GSE85600.

Differentially expressed genes were tested for enrichment using gene set enrichment analysis (GSEA) from MSigDB (http://www.broad.mit.edu/gsea/; ref. 12). Gene expression signatures, specifically up or downregulated in human B-ALL gene sets (13, 14), were assessed for their overlap with up or downregulated genes within tumor specimen, using GSEA enrichment analysis. Moreover enrichment analysis for the specific normal murine B-cell stage signatures (15), BCR-ABL signature (16), BCR-ABL target genes (obtained from http://www.broad.mit.edu/gsea/) and for the specific *Pax5* gene signatures described in (17–20) were carried out.

Cloning of Hek293T constructs

A cDNA encoding the CDS of the wild-type murine *Pax5* was obtained from the Pax5 Plasmid (#35003; Addgene; ref. 21) via PCR using the Phusion High-Fidelity DNA Polymerase (Thermo Scientific). The mutant cDNAs for murine *Pax5* (P80R, P80L, R38C, P32L, I54N, V26G) were created by site directed mutagenesis by PCR with the same polymerase. The obtained *Pax5* sequences were cloned into a derivative of a bicistronic expression vector (pMC3) used previously for stable expression of genes in cell lines (22). Here, the vector was modified to encode the Hygromycin resistance gene as the second cistron (pMC3-PAX5.Hygro). The identity of the respective cDNAs was confirmed by Sanger sequencing.

Hek293T cells were transfected using the Attractene Transfection Reagent (Qiagen), according to manufacturer's protocol. Briefly, 1.2 μg of each pMC3-PAX5.Hygro construct or the empty vector was diluted in 100 μL serum-free media, before 4.5 μL of Attractene was added. After an incubation period of 15 minutes the DNA/Attractene mix was added to Hek293T cells (6×10^5) in suspension and plated on a six-well plate. Cells harboring the plasmids were selected using 200 μg/mL Hygromycin B (Life Technologies).

Downloaded from http://aacrjournals.org/cancerres/article-pdf/78/10/2669/2764846/2669.pdf by guest on 05 February 2024

Luciferase assay

Hek293T cells expressing pMC3-PAX5.Hygro^{WT}, pMC3-PAX5.Hygro^{Empty}, or pMC3-PAX5.Hygro^{mutant} were transfected with 2 μg *luc-CD19* construct (kindly provided by M. Busslinger; ref. 23) and 100 ng pRL-TK *Renilla* luciferase plasmid DNA (Promega) using FuGene 6 (Roche Diagnostics). Fourty-eight hours after transfection, cells were lysed and *Firefly* and *Renilla* luciferase activity measurement was performed using the Dual-Glo Luciferase Assay System (Promega), according to manufacturer's protocol. All transfections were carried out in triplicate in at least three independent experiments. *Firefly* luciferase activity was normalized according to the corresponding *Renilla* luciferase activity.

Immunoblot analysis

B220$^+$ BM cells of healthy Sca1-BCR-ABL^{P190} and Sca1-BCR-ABL^{P190}+*Pax5*$^{+/-}$ mice were FACS sorted, while Ba/F3 cells expressing BCR-ABL^{P190} served as a positive control (24). Cells were lysed in RIPA buffer (50 mmol/L Tris pH 8.0, 150 mmol/L NaCl, 0.5% sodiumdeoxycholate, 1% NP-40 substitute, 0.1% SDS), containing protease and phosphatase inhibitors (Roche Diagnostics). Twenty micrograms of whole protein was separated on SDS-PAGE and transferred to Hybond-C Extra membranes (Amersham Biosciences). Immunoblotting was carried out using the following antibodies: c-ABL 1:1000 (Cell Signaling Technology, #2862), p-STAT5 1:1000 (Cell Signaling Technology, mAb #9359), STAT5 1:1000 (mAb #9358; Cell Signaling Technology), and β-actin clone AC-74 1:10000 (Sigma-Aldrich). Detection was carried out using anti-rabbit or anti-mouse horseradish peroxidase conjugates (Santa Cruz Biotechnology), respectively, with an ECL system (Thermo Scientific).

Western blot analysis of BCRABL^{P190} expression and presence of pCrkL (Tyr207) was carried out in control and leukemic Sca1-BCR-ABL^{P190}+*Pax5*$^{+/-}$ cells cultured in the presence of IL7. As positive controls, we used the following cell lines: Ba/F3+BCRABL^{P190}, a Ba/F3 cell line expressing human BCRABL^{P190} (24), and TOM-1 cells that were established in 1983 from the bone marrow of a 54-year-old woman with refractory Philadelphia chromosome-positive acute lymphoblastic leukemia (ALL; ref. 25). All cells were maintained in RPMI with 10% FCS. Extracts were normalized for protein content by Bradford analysis (BioRad Laboratories Inc.). The following primary antibodies were used: BCR (Ab2; Oncogene Science), pCrkL (Tyr207; Cell Signaling) and β-actin (I19; Santa Cruz Biotechnology). Reactive bands were detected with an ECL system (Amersham).

Glucose, lactate, and ATP measurements

Glucose and lactate levels were measured using the Amplex Red Glucose/Glucose Oxidase Assay Kit (Invitrogen) and the L-Lactate Assay Kit (Cayman Chemical), respectively, according to the manufacturers' protocols. Glucose and lactate concentrations were measured in fresh and spent medium. Total ATP levels were measured using the ATP Bioluminescence Assay Kit CLS II (Roche) according to the manufacturer's protocol. One million cells per mL were seeded in fresh medium. Relative levels of glucose consumed, lactate produced and total ATP are shown. To account for different rates of cell proliferation and death, all three parameters were normalized to number of viable cells as determined by applying Trypan blue exclusion.

Metabolic assays using the XFe24 flux analyzer

Glycolytic profiles were monitored under basal conditions (glycolytic activity) and in response to acute addition of oligomycin (an inhibitor of ATP synthase). Glycolytic activity was measured as extracellular acidification rate (ECAR). Oligomycin suppresses mitochondrial ATP production, leading to increased compensatory glycolysis to meet the energy demands of the cell and to maintain energy homeostasis. This elevated rate of glycolysis is called glycolytic capacity. ECAR was measured using a Seahorse XFe24 Flux Analyzer (Seahorse Bioscience). Briefly, 1.5×10^5 cells per well were plated using Cell-Tak (BD Biosciences). Prior to measurements, cells were incubated in XF Base Medium supplemented with 25 mmol/L glucose, 1 mmol/L sodium pyruvate, and 2 mmol/L GlutaMAX for 1 hour at 37°C (non-CO_2 incubator) for pH stabilization. ECAR was measured at the resting stage (glycolytic activity in XF Base Medium supplemented with glucose, sodium pyruvate, and GlutaMax) and in response to oligomycin (1 μmol/L; glycolytic capacity). Oxygen consumption rate (OCR) was measured using a Seahorse XFe24 Flux Analyzer with the XF Cell Mito Stress Test Kit (Seahorse Bioscience) according to the manufacturer's instructions. OCR was measured in response to oligomycin (1 μM). All parameters were normalized to number of viable cells as determined by applying Trypan blue exclusion.

Chromatin immunoprecipitation sequencing analysis

Chromatin immunoprecipitation sequencing (ChIP-seq) tracks for PAX5 antibodies in human B lymphocytes (ENCODE, Encyclopedia of DNA Elements, GM12878) are downloaded from: http://genome.ucsc.edu/ENCODE/dataMatrix/encodeChipMatrixHuman.html. Gene models are shown in UCSC genome browser hg19.

Results

Limiting BCR-ABL^{P190} expression to HS/PCs induces pB-ALL with reduced penetrance

To explore early cellular changes in BCR-ABL^{P190} preleukemic HS/PCs that might take place in the development of BCR-ABL^{P190}-pB-ALL, we engineered mice with restricted oncogene expression to HS/PCs by placing the *BCR-ABL*^{P190} cDNA under the control of the Sca1 (stem cell antigen 1) promoter (Sca1-BCR-ABL^{P190}; Supplementary Fig. S1A; refs. 10, 26). Insertion of the *TK-IRES-BCR-ABL*^{P190} cDNA under the control of the mouse Ly-6E.1 promoter (9) yielded the plasmid Sca1-*BCR-ABL*^{P190} (Supplementary Fig. S1A), which was used to drive Sca1-directed expression of BCR-ABL^{P190} in C57BL/6 × CBA mice. Two founder lines were obtained for the *Sca1-BCR-ABL*^{P190} transgene, which were viable, developed normally and were used for further studies. The BCR-ABL^{P190} transcript was only detected in Sca1$^+$Lin$^-$ cells (Fig. 1A) and expression and signaling of the fusion protein was absent in healthy B220$^+$ sorted bone marrow (BM) cells of BCR-ABL^{P190} mice as shown by Western blot and GSEA analyses (B). To further assess the developmental stage at which Sca1-BCR-ABL^{P190} expression was downregulated, qRT-PCR detection of the transgene was carried out in HS/PC populations of the respective healthy mice. These data confirmed a drastic decrease of *BCR-ABL*^{P190} expression, starting at the stage of common lymphoid progenitors, whereas the transgene could no longer be detected at the level of pro-B cells (Supplementary Fig. S1B).

Downloaded from http://aacrjournals.org/cancerres/article-pdf/78/10/2669/2764846/2669.pdf by guest on 05 February 2024

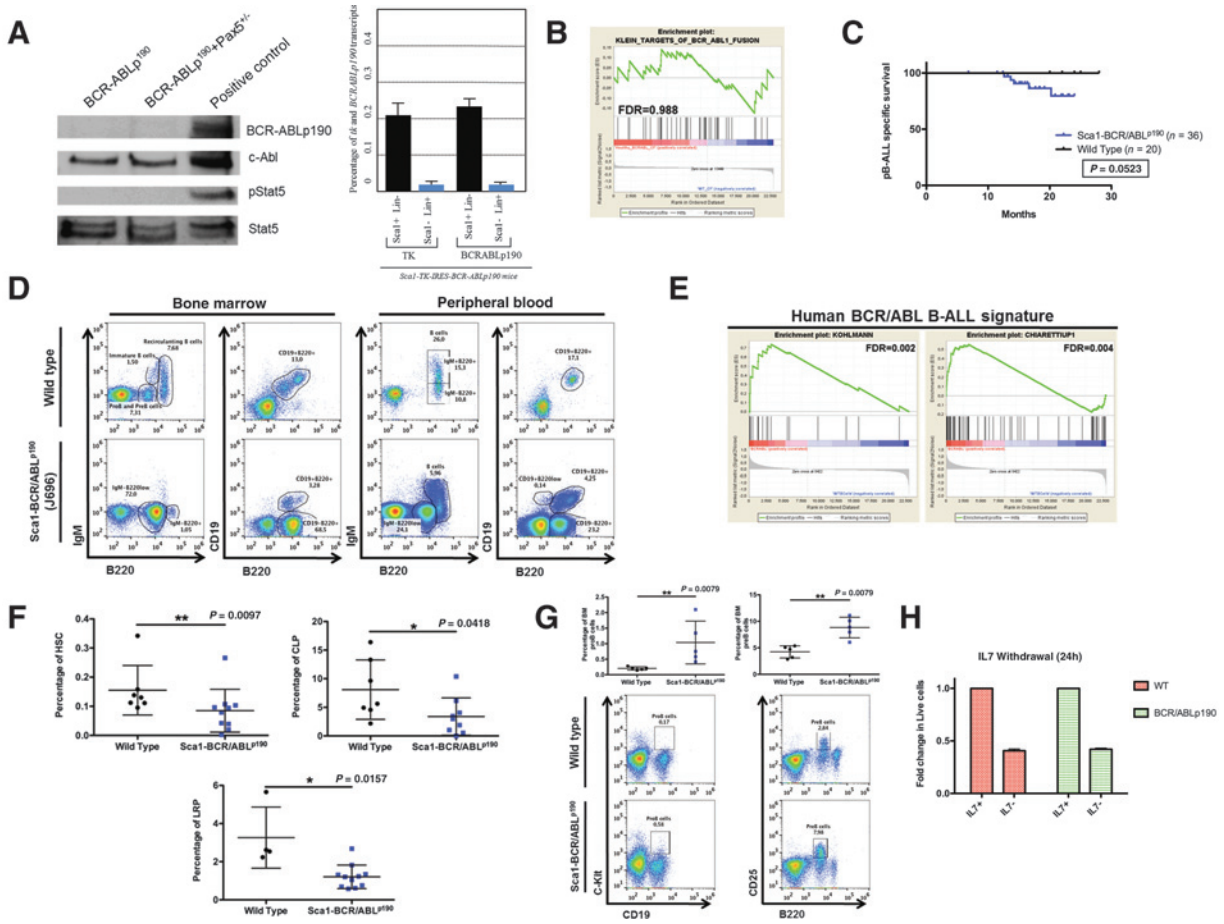

Figure 1.

Transient BCR-ABL^{p190} expression in HS/PCs is sufficient to induce pB-ALL. **A,** BCR-ABL^{p190} is absent in precursor B-cells of preleukemic Sca1-BCR-ABL^{p190} and Sca1-BCR-ABL^{p190}+*Pax5*$^{+/-}$ mice. Left, B220-positive cells from the BM of preleukemic Sca1-BCR-ABL^{p190} and Sca1-BCR-ABL^{p190}+*Pax5*$^{+/-}$ mice were FACS sorted, and lysates were subjected to immunoblot analysis for c-Abl, as well as p-Stat5, and total Stat5. Ba/F3+BCRABL^{p190} cells served as positive control. One representative experiment out of two biological replicates is shown. Right, quantification of thymidine kinase (TK) and BCR-ABL^{p190} expression in Sca1-BCR-ABL^{p190} mice by real-time PCR in Sca1^{+}Lin^{-} and Sca1^{-}Lin^{+} cells. The percentage of TK and BCR-ABL^{p190} transcripts with reference to β-actin is shown. **B,** GSEA analysis showing BCR-ABL target genes are not enriched in preleukemic pro-B/pre-B cells of Sca1-BCR-ABL^{p190} mice compared with pro-B/pre-B cells of wild-type (WT) mice age-matched [false discovery rate (FDR) = 0.988]. **C,** pB-ALL specific survival curve of Sca1-BCR-ABL^{p190} mice (blue; $n = 36$) compared with WT control mice (black; $n = 20$; log-rank P value = 0.0523). **D,** Flow cytometric analysis of hematopoietic subsets in diseased Sca1-BCR-ABL^{p190} mice. Representative plots of cell subsets from the BM and PB show accumulation of blast B cells in Sca1-BCR-ABL^{p190} mice ($n = 5$) compared with control littermate WT mice age-matched ($n = 5$). **E,** GSEA of leukemic mice. GSEA identified significant enrichment in human BCR-ABL pB-ALL gene sets (extracted from refs. 13, 14) in Sca1-BCR-ABL^{p190} tumor-bearing BMs compared with B220^{+} BM B cells from WT mice (GSEA FDR = 0.002 and FDR = 0.004). **F,** Percentage of HSC, CLP, and LRP in 4-month-old Sca1-BCR-ABL^{p190} mice ($n = 9$–11) compared with age-matched WT mice ($n = 4$–7) analyzed by flow cytometry. Error bars, SD. Unpaired t test P value is indicated in each case. **G,** Percentage of BM pro-B cells in 4-month-old Sca1-BCR-ABL^{p190} mice ($n = 5$) compared with age-matched WT mice ($n = 5$) analyzed by flow cytometry. Error bars, SD. Unpaired t test P value is indicated in each case. Representative flow cytometry plots of pro-B cell subsets are shown at the bottom. **H,** Cell death susceptibility mediated by IL7 removal in Sca1-BCR-ABL^{p190} pro-B cells. Sorted B220^{+} cells from BM of young Sca1-BCR-ABL^{p190} and WT mice were cultured under conditions to allow the isolation and expansion of a pure population of pro-B cells. Pro-B cells were cultured with or without IL7 for 24 hours. Induction of apoptosis was assessed by flow cytometry using Annexin V/PI staining. Data represent the means ± SD of normalized live cells from six independent experiments.

In an aging mouse colony, Sca1-BCR-ABL^{p190} mice developed pB-ALL with low penetrance (13%), with earliest disease occurrence at 13 months (Fig 1C). The leukemia was characterized by blast infiltration, appearance of blast B-cells (CD19^{-}B220^{+}IgM^{-}) in BM and peripheral blood (PB) and disruption of splenic architecture (Fig. 1D; Supplementary Fig. S1C). Transcriptome analysis revealed that these Sca1-BCR-ABL^{p210} pB-ALLs were aligned with the pro-B/pre-B cell stage (Supplementary Fig. S1D; refs. 12, 15) and resembled the human BCR-ABL^{p190}-pB-ALL signature, despite the absence of BCR-ABL^{p190} in the blast cells (Fig. 1E; refs. 13, 14). In accordance with this observation, BCR-ABL signaling was not enriched in leukemic Sca1-BCR-ABL^{p190} cells (Supplementary Fig. S1e). Therefore, these data demonstrate that limited expression of the BCR-ABL^{p190} oncogene in HS/PCs is capable of inducing pB-ALL. Moreover, the resulting pB-ALLs align with a differentiation stage comparable to human BCR-ABL^{p190}-pB-ALL, while being independent of a detectable BCR-ABL^{p190} oncogene expression and activation of its downstream signaling.

Downloaded from http://aacrjournals.org/cancerres/article-pdf/78/10/2669/2764846/2669.pdf by guest on 05 February 2024

Pax5-defective pro-B/pre-B cells are permissive for Sca1-BCR-ABL^{P190} pB-ALL development

To elucidate the mechanism underlying this specific BCR-ABL^{P190}-mediated pB-ALL susceptibility, we analyzed the different B-cell developmental stages in healthy Sca1-BCR-ABL^{P190} and WT littermates of the same breeding. Healthy Sca1-BCR-ABL^{P190} mice showed reduced numbers of hematopoietic stem cells (HSC), common lymphoid progenitors (CLP), and lineage restricted progenitors (LRP) compared with WT controls, whereas the percentage of pro-B/pre-B cells in the BM was significantly increased (Fig. 1F and G; Supplementary Fig. S1F and S1G; Supplementary Table S1). Serial blood analysis revealed that although healthy Sca1-BCR-ABL^{P190} mice exhibited higher B220^{+} cell numbers at 2 months of age, their B cells rapidly decrease and level off below 20% around 6 months after birth (Supplementary Fig. S2A and S2B). Murine precursor B-cells are dependent on intact IL7/IL7R signaling, thus we explored the response of healthy Sca1-BCR-ABL^{P190} pro-B cells to IL7 withdrawal. In agreement with the lack of BCR-ABL^{P190} signaling in the respective cells, our findings showed that these cells are similar sensitive to IL7 withdrawal as their WT counterparts (Fig. 1H). Therefore, these data suggest that BCR-ABL^{P190} favors the appearance of an aberrant precursor B-cell compartment in the BM and that differentiation to mature B cells is impaired without exposure of the precursor B cells to the oncogenic BCR-ABL^{P190} kinase. Thus, we hypothesized that the nature and function of the second hit must determine the specific target cell expansion. In addition to the absence of the B-cell marker CD19, Pax5 transcriptional activity was lost or markedly reduced in leukemic cells of Sca1-BCR-ABL^{P190} pB-ALLs (Supplementary Tables S2 and S3; Supplementary Fig. S2C). These findings suggested Pax5 as a candidate for a second oncogenic hit, because as a master regulator of B-cell development and identity (8), *PAX5* loss-of-function alterations occur in around 30% of human BCR-ABL^{P190} B-ALL (27). To investigate the functional consequence of combined reduction of Pax5 dosage and restricted BCR-ABL^{P190} expression in HS/PCs, we generated Sca1-BCR-ABL^{P190}+*Pax5*$^{+/-}$ mice. In line with the results from Sca1-BCR-ABL^{P190} only mice, these mice also displayed absence of the BCR-ABL^{P190} fusion protein in healthy B220^{+} BM cells and inactive BCR-ABL^{P190} downstream signaling (Figs. 1A and 2A). Sca1-BCR-ABL^{P190}+*Pax5*$^{+/-}$ mice did not display a decrease in the total number of pro-B cells; however, the number of B220^{+} cells in the PB was reduced directly after birth and their IL7 sensitivity was increased, comparable to pro-B cells of *Pax5*$^{+/-}$ mice (Fig. 2B and C; Supplementary Fig. S2A and S2B; ref. 22). Compared with Sca1-BCR-ABL^{P190} mice, Sca1-BCR-ABL^{P190}+*Pax5*$^{+/-}$ mice developed pB-ALL with higher incidence (90%) and earlier disease onset (Fig. 2D). The same pB-ALL development could be observed, when cells from Sca1-BCR-ABL^{P190}+*Pax5*$^{+/-}$ mice were transplanted into sublethally irradiated syngeneic mice, while no leukemia developed from Pax5$^{+/-}$ wild-type pro-B cells (Supplementary Fig. S3A–S3C). Because the development of pB-ALL in *Pax5* heterozygous mice was recently linked to infection exposure (22), Sca1-BCR-ABL^{P190}+*Pax5*$^{+/-}$ cohorts were kept in a conventional as well as a specific pathogen free (SPF) facility, in order to address whether infection plays a role for leukemia initiation. Both cohorts developed pB-ALL at comparable rates (Supplementary Fig. S4A and S4C), which highlights the fact that in the Sca1-BCR-ABL^{P190}+*Pax5*$^{+/-}$ model, Pax5 does not function as a susceptibility event in pB-ALL development.

In addition, the blast population of the pB-ALLs from Sca1-BCR-ABL^{P190}+*Pax5*$^{+/-}$ mice lacked BCR-ABL^{P190} activity (Fig. 2E; Supplementary Fig. S5A). In line with these results, neither BCR-ABL^{P190} protein nor downstream signaling was detected in leukemic Sca1-BCR-ABL^{P190}+*Pax5*$^{+/-}$ cells (Supplementary Fig. S5B), which is further supported with resistance of the murine Sca1-BCR-ABL^{P190}+*Pax5*$^{+/-}$ leukemic cells to Gleevec treatment (Supplementary Fig. S5C). The blast population was clonal, with a cell surface phenotype of CD19^{-}B220^{+}IgM^{-}Mac1$^{+/-}$ and accumulated in the BM, PB, lymph nodes, and spleen (Fig. 2F; Supplementary Fig. S5D and S5E). Moreover, isolated leukemic pro-B cells were able to grow independent of IL7 (Fig. 2G). Sca1-BCR-ABL^{P190}+*Pax5*$^{+/-}$ leukemic gene expression profiles clustered together with those of Sca1-BCR-ABL^{P190} leukemias and classified Sca1-BCR-ABL^{P190}+*Pax5*$^{+/-}$ pB-ALLs as pro-B cell stage (Supplementary Fig. S5F and S5G). These results suggest that even without active BCR-ABL^{P190} expression, the pB-ALL cells of Sca1-BCR-ABL^{P190}+*Pax5*$^{+/-}$ mice closely resemble the human BCR-ABL pB-ALL signature (Supplementary Fig. S5H). Moreover, they showed downregulation of genes important for B-cell development and differentiation, including *Pax5*, *Ikzf1*, and *CD19* (Supplementary Table S4), which was confirmed by lost or markedly reduced Pax5 transcriptional activity in Sca1-BCR-ABL^{p190}+*Pax5*$^{+/-}$ leukemic cells (Supplementary Fig. S5I). To rule out that the heterogeneity of the control B cells could also contribute to the observed differential gene expression pattern, we characterized the global expression signature of purified wild-type pro-B/pre-B cells and compared with the expression signature of leukemic Sca1-BCR-ABL^{P190}+*Pax5*$^{+/-}$ and Sca1-BCR-ABL^{P190} cells. The analysis showed similar differential gene expression profile and similar GSEA enrichments than when it was compared with BM B220^{+} cells [Supplementary Fig. S5F (bottom); Supplementary Fig. S5J–K].

Taken together, the characteristics of Sca1-BCR-ABL^{P190}+*Pax5*$^{+/-}$ pB-ALLs overlap to a large extent with the observations in Sca1-BCR-ABL^{P190} leukemias. However, the increase in pB-ALL incidence and reduced latency without affecting the incidence of myeloid and nonhematopoietic tumors suggest that the time point and cellular compartment in which the *Pax5* mutations take place facilitate and determine to a large extent the clonal evolution of Sca1-BCR-ABL^{P190} mediated pB-ALL development.

Identification of *Pax5* as a barrier of clonal selection in Sca1-BCR-ABL^{P190} pB-ALL development by next-generation sequencing

To validate these findings on a genomic level, as well as to further identify somatically acquired second hits leading to pB-ALL development, we performed whole exome sequencing of three Sca1-BCR-ABL^{P190} and 13 Sca1-BCR-ABL^{P190}+*Pax5*$^{+/-}$ BM tumor samples and their corresponding germline samples. The resulting somatic variants revealed that *Jak3* and *Pax5* genes were recurrently mutated in Sca1-BCR-ABL^{P190}+*Pax5*$^{+/-}$ pB-ALLs, whereas Sca1-BCR-ABL^{P190} only tumors displayed a heterogeneous mutational spectrum (Supplementary Fig. S6A and S6B; Supplementary Table S3). For the *Pax5* gene, a variety of different *Pax5* mutations were found in 46% of Sca1-BCR-ABL^{P190}+*Pax5*$^{+/-}$ mice, which were all located in the gene's DNA binding domain (Fig. 3A).

Given that *Pax5* p.P80R and p.V26G result in reduced PAX5 activity in humans (27, 28), we performed reporter gene assays to further assess the functional consequences of the newly identified

Downloaded from http://aacrjournals.org/cancerres/article-pdf/78/10/2669/2764846/2669.pdf by guest on 05 February 2024

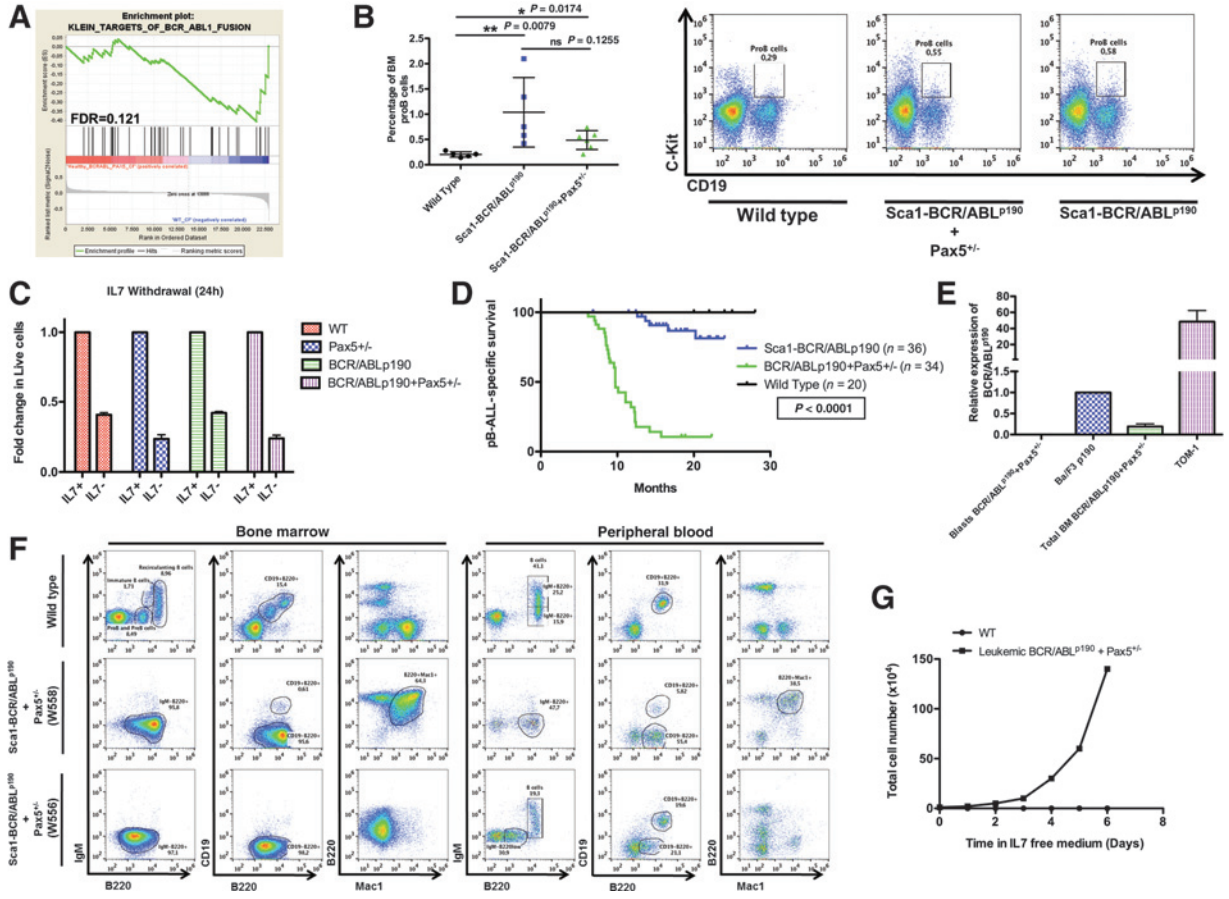

Figure 2.

Pax5-defective pro-B/pre-B cells are permissive for BCR-ABL^{p190} pB-ALL development, as shown in Sca1-BCR-ABL^{p190}+*Pax5*$^{+/-}$ mice. **A,** GSEA analysis showing BCR-ABL target genes are not enriched in preleukemic pro-B/pre-B cells of Sca1-BCR-ABL^{p190}+*Pax5*$^{+/-}$ mice compared with pro-B/pre-B cells of WT mice age-matched [false discovery rate (FDR) = 0.121]. **B,** Percentage of BM pro-B cells in 4-month-old Sca1-BCR-ABL^{p190}+*Pax5*$^{+/-}$ mice ($n = 5$) compared with age-matched Sca1-BCR-ABL^{p190} ($n = 5$) and WT mice ($n = 5$) analyzed by flow cytometry. Error bars, SD. Unpaired *t* test *P*-value is indicated in each case. Representative flow cytometry plots of pro-B cell subsets are shown on the right. ns, nonsignificant. **C,** Cell death susceptibility mediated by IL7 removal in Sca1-BCR-ABL^{p190}+*Pax5*$^{+/-}$ pro-B cells. Sorted B220^{+} cells from BM of young Sca1-BCR-ABL^{p190}+*Pax5*$^{+/-}$, Sca1-BCR-ABL^{p190}, *Pax5*$^{+/-}$, and WT mice were cultured under conditions to allow the isolation and expansion of a pure population of pro-B cells. Pro-B cells were cultured with or without IL7 for 24 hours. Induction of apoptosis was assessed by flow cytometry using Annexin V/PI staining. Data represent the means ± SD of normalized live cells from six independent experiments. **D,** pB-ALL–specific survival curve of Sca1-BCR-ABL^{p190}+*Pax5*$^{+/-}$ mice (green; $n = 34$) compared with Sca1-BCR-ABL^{p190} (blue; $n = 36$) and WT control mice (black; $n = 20$) showing a significantly (log-rank $P < 0.0001$) shortened life span. **E,** Relative expression of BCR-ABL^{p190} in total BM of a leukemic WT mouse transplanted with Sca1-BCR-ABL^{p190}+Pax5$^{+/-}$ proB cells, total bone marrow of preleukemic Sca1-BCR-ABL^{p190}+Pax5$^{+/-}$ mice and TOM-1 cell line, respectively. A Ba/F3+BCR-ABL^{p190} (Ba/F3^{p190}) cell line was used as a positive control. Error bars, mean ± SD of three replicates. **F,** Flow cytometric analysis of hematopoietic subsets in diseased Sca1-BCR-ABL^{p190}+*Pax5*$^{+/-}$ mice. Representative plots of cell subsets from the BM and PB show accumulation of blast B cells in Sca1-BCR-ABL^{p190}+*Pax5*$^{+/-}$ mice ($n = 27$) compared with control littermate WT mice age-matched ($n = 5$). **G,** WT and leukemic Sca1-BCR-ABL^{p190}+*Pax5*$^{+/-}$ primary cells were cultured in media without IL7. Proliferation was measured using Trypan blue. Values represent the mean of three replicates with essentially identical datasets.

Pax5 variants. The Pax5-dependent reporter gene assay (23) showed significant reduction of all Pax5 variants in transcriptional activation compared with WT Pax5 (Fig. 3B). Moreover, whole genome sequencing revealed an additional wide-range deletion of *Pax5* Exon 2–4 in one Sca1-BCR-ABL^{P190}+*Pax5*$^{+/-}$ mouse (W556), whereas similar deletions were detected in two additional Sca1-BCR-ABL^{P190}+*Pax5*$^{+/-}$ mice without *Pax5* variant (S650 and S314) by PCR (Fig. 3C). Therefore, these data suggest that reduction/loss of wild-type Pax5 played a significantly role in disease development. To further monitor disease evolution over time, we performed deep sequencing of the *Pax5* variant p.I54N with a read depth up to 2 million reads using bleedings of the corresponding mouse. *Pax5* p.I54N was first detectable in the leukemic sample (Fig. 3D), whereas it was absent in the sample taken prior to disease development, emphasizing the relevance of aberrant Pax5 expression for disease progression. This indicates that during the early lifespans of mice, the pre-B cell population initiates polyclonal VDJ recombination events from which a monoclonal leukemia will emerge later in life. In agreement with this, polyclonal VDJ recombination events were evident in this preleukemic pre-B cell population from which monoclonal pre-B leukemia can emerge (Supplementary Fig. S7A and S7B). Taken together, these data show that in order to achieve clonal selection for BCR-ABL^{P190}-mediated pB-ALLs, elimination or significant reductions of wild-type Pax5 activity is critical for disease progression.

Downloaded from http://aacrjournals.org/cancerres/article-pdf/78/10/2669/2764846/2669.pdf by guest on 05 February 2024

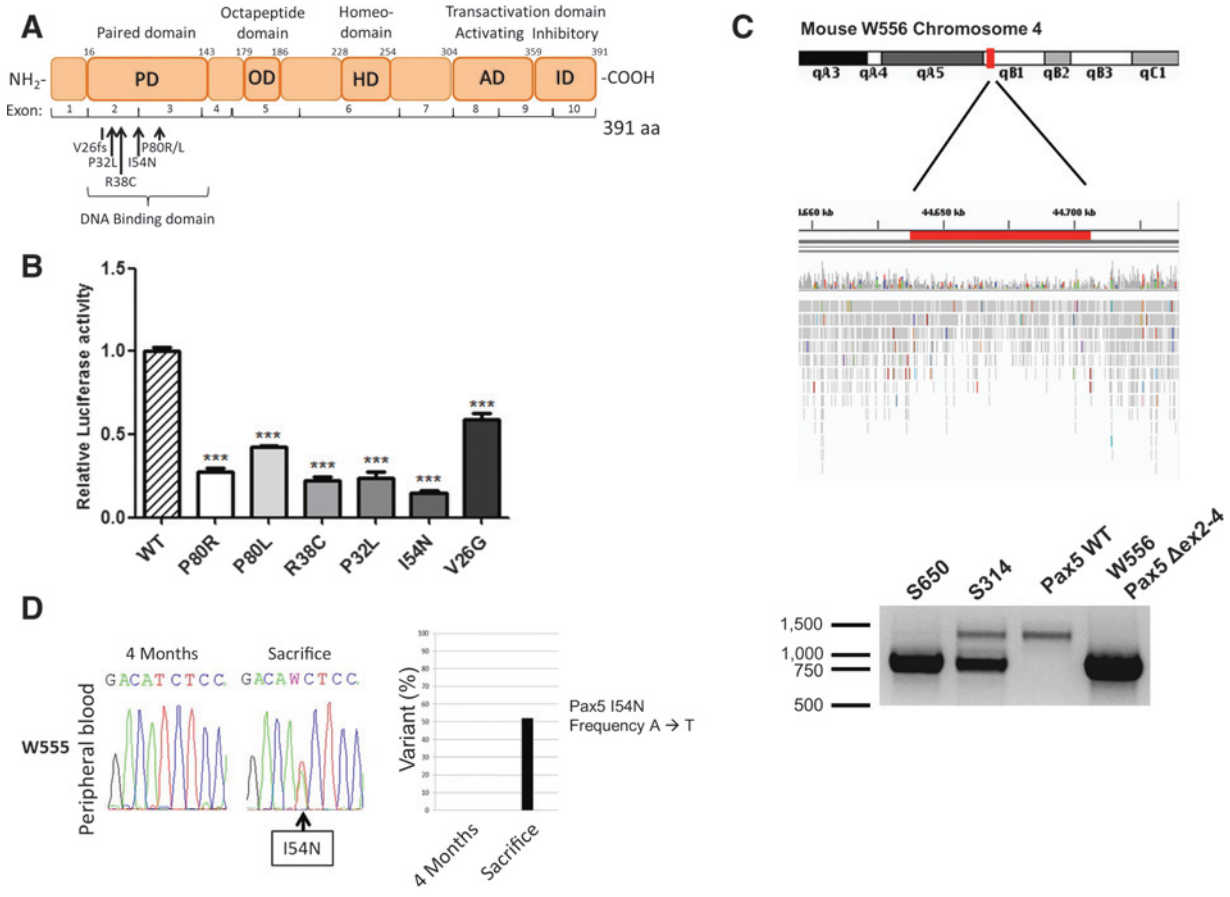

Figure 3.

Mouse tumor exome sequencing data identify the second hit within the WT *Pax5* gene. **A,** Schematic of *Pax5* gene domains. Displayed are single nucleotide variants identified by whole exome sequencing in Sca1-BCR-ABL^{p190}+*Pax5*$^{+/-}$ mice, which are all located in the gene's DNA binding domain. **B,** Attenuated transcriptional activity of Pax5^{mutant} proteins. Relative luciferase activity is indicated for Pax5^{WT} and Pax5^{mutant} proteins, as measured by a Pax5-dependent reporter gene assay in Hek293T cells, which were stably transfected with the different Pax5 constructs. Bars show mean luciferase activity from three individual experiments with triplicate measurements. ***, $P < 0.0001$, as calculated by Dunnett test. **C,** Top, whole genome analysis identifies a deletion spanning more than 27 kb in the *Pax5* gene on Chromosome 4 in mouse W556 (red). Bottom, *Pax5* deletion analysis on cDNA level reveals two additional Pax5 truncations in mice S650 and S314 (similar to that observed in mouse W556). Whole BM cDNA from a healthy *Pax5*$^{+/-}$ mouse (WT) served as control. **D,** Backtracking of I54N in the murine *Pax5* gene by Sanger and Amplicon sequencing, using genomic DNA of bimonthly bleedings of Sca1-BCR-ABL^{p190}+*Pax5*$^{+/-}$ mouse W555. The leukemic clone is only detectable in the diseased mouse at around 5 months (sacrifice) of age ($n = 2$).

Reduced Pax5 activity drives the metabolic switch toward glucose utilization and energy metabolism in Sca1-BCR-ABL^{P190} leukemia

To elucidate the underlying mechanism by which reduced Pax5 activity mediates disease progression, transcriptome analyses were performed, which showed enrichment in genes expressing mediators of glucose uptake and utilization, as well as energy metabolism in both Sca1-BCR-ABL^{P190} and Sca1-BCR-ABL^{P190}+*Pax5*$^{+/-}$ pB-ALL cells, when compared with WT cells (Fig. 4A; Supplementary Fig. S8–S10). To investigate the clinical relevance of our findings and to determine whether human pB-ALLs share a similar metabolic signature, we studied gene expression data from human pB-ALLs as well as normal pro-B, pre-B-I, pre-B-II, and immature B cells (29, 30). As expected, expression of *PAX5* was downregulated in human pB-ALLs (Supplementary Fig. S11). In contrast, several metabolic genes (*IDH1*, *G6PC3*, *GAPDH*, *PGK1*, *HK3*, *MYC*, *ENO1*, and *ACO1*) were upregulated in both our mouse pB-ALL models (Fig. 4A) and human pB-ALL cells (Supplementary Fig. S11; refs. 29, 30). The metabolic genes identified play key roles in modulating glucose utilization and energy metabolism. Hexokinases mediate the first committed step in most glucose metabolism pathways (31), and *HK3* is a transcriptional target of the myeloid transcription factor *CEBPA*, which opposes B-cell transcription factors (32). Glyceraldehyde 3-phosphate dehydrogenase (*GAPDH*), phosphoglycerate kinase (*PGK1*), and enolase 1 (*ENO1*) catalyze distinct steps of glycolysis (33). *G6PC3* encodes the catalytic subunit of glucose-6-phosphatase that mediates the last step of gluconeogenic and glycogenolytic pathways (34). Isocitrate dehydrogenase 1 *(IDH1*) and acotinase 1 (*ACO1*) are essential enzymes in the tricarboxylic acid cycle, which plays a critical role in energy metabolism (35). Furthermore, *MYC*-driven transformation leads to increased expression of glycolytic enzymes and glucose utilization (36). Notably, analysis of ChIP-seq data obtained using human B lymphocytes (ENCODE GM12878) revealed that PAX5 binds to the promoter region of *IDH1*, *G6PC3*, *GAPDH*, *PGK1*, *MYC1*,

Downloaded from http://aacrjournals.org/cancerres/article-pdf/78/10/2669/2764846/2669.pdf by guest on 05 February 2024

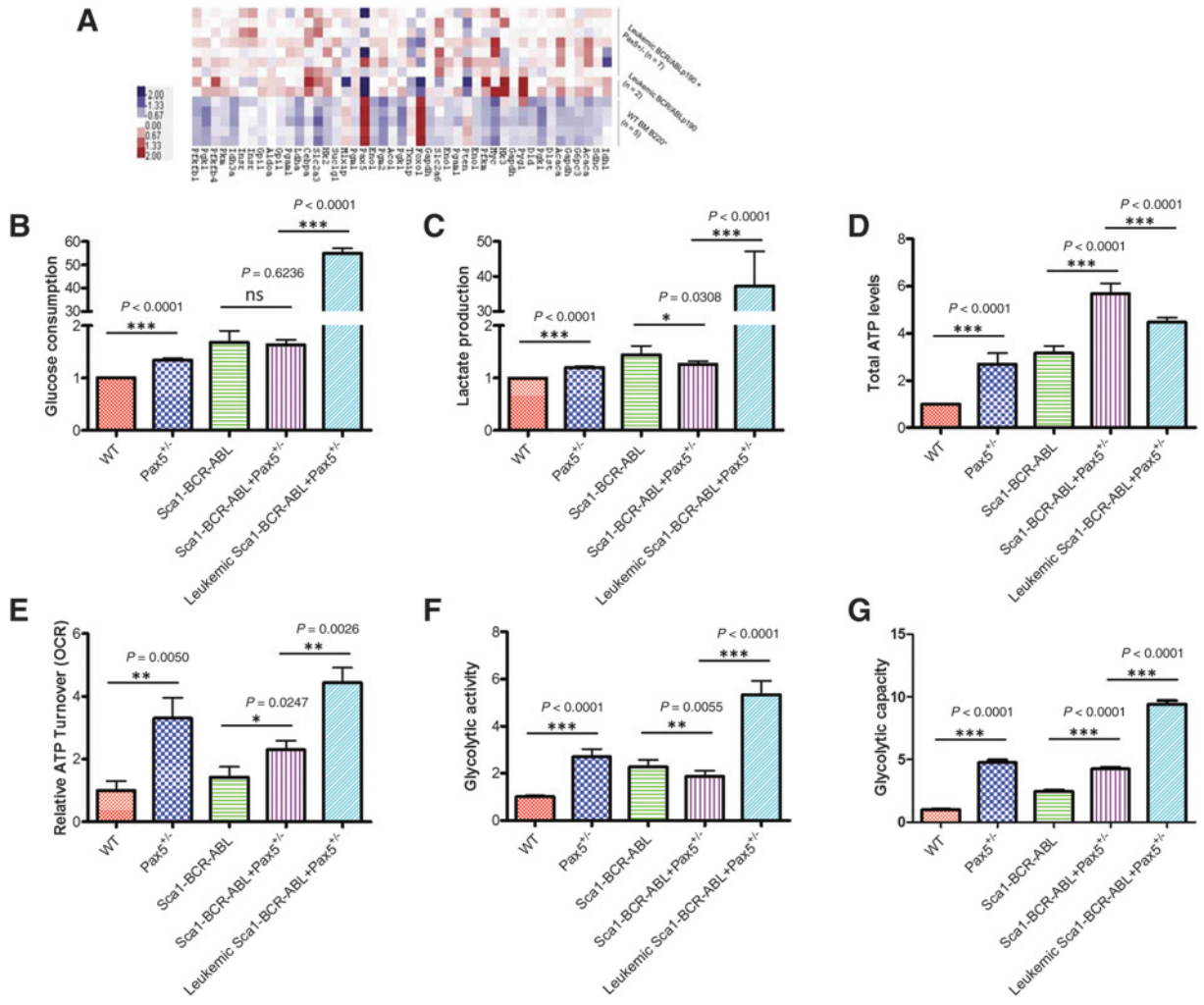

Figure 4.

Glycolytic energy production in Sca1-BCR-ABL^{p190}-negative leukemic pro-B cells. **A,** Gene expression changes in regulators of glucose uptake and energy supply in leukemic Sca1-BCR-ABL^{p190} ($n = 2$), Sca1-BCR-ABL^{p190}+*Pax5*$^{+/-}$ ($n = 7$), and WT BM B220^{+} cells ($n = 5$) were plotted as heat map. **B–G,** Metabolic measurements were performed for (i) *Pax5* WT pro-B, (ii) *Pax5* WT; Sca1-BCR-ABL^{p190} pro-B (nonleukemia), (iii) *Pax5*$^{+/-}$ pro-B, (iv) *Pax5*$^{+/-}$; Sca1-BCR-ABL^{p190} pro-B (non-leukemic), and (v) *Pax5*$^{+/-}$; Sca1-BCR-ABL^{p190} leukemia cells. For measurements of glucose consumption ($n = 6$; **B**), lactate production ($n = 6$; **C**), and total ATP levels ($n = 6$; **D**), cells were seeded in fresh medium. On day 3 following seeding of cells, cells and spent medium were harvested and processed for metabolic measurements. **E–G,** Oxygen consumption rate (OCR) was measured to monitor mitochondrial ATP turnover ($n = 3$; **E**). ECAR were measured at the resting state (with glucose; glycolytic activity; $n = 6$; **F**) and in response to oligomycin (glycolytic capacity; $n = 6$; **G**). All values are normalized to cell numbers and are shown as average amounts relative to average values of WT control (±SD). *P* values are indicated as calculated by the Student *t* test.

ENO1, and *ACO1* (Supplementary Fig. S12). PAX5 can function as a transcriptional activator and a repressor through interaction with Groucho family factors (37). These findings suggest that loss of *PAX5* function may drive metabolic reprogramming during disease progression through transcriptional regulation of these metabolic genes.

To elucidate the functional significance of gene expression changes observed in our models, metabolic assays were performed to characterize Sca1-BCR-ABL^{p190}- and PAX5-mediated metabolic reprogramming in our models. Consistent with the metabolic signature observed, significant increases in levels of glucose consumed (~55-fold), lactate produced (~37-fold), and total ATP (~16-fold) were drastically increased in Sca1-BCR-ABL^{p190}+*Pax5*$^{+/-}$ leukemic cells compared with their normal counterpart (Fig. 4B–D). Furthermore, increases in glycolytic activity (~5- to 6-fold), glycolytic capacity (~9- to 10-fold) and mitochondrial ATP production (~4-fold; Fig. 4E–G) were observed in Sca1-BCR-ABL^{p190}+*Pax5*$^{+/-}$ leukemic cells. Metabolic measurements also revealed that glucose consumption (~1.7-fold), lactate production (~1.4-fold), and total ATP levels (~3-fold) were increased in non-leukemic Sca1-BCR-ABL^{p190} pro-B cells carrying WT *Pax5* (Fig. 4B–D). Similarly, increased glucose consumption (~1.3-fold), lactate production (~1.2-fold), and total ATP levels (~3-fold) were observed in *Pax5*-deficient pro-B cells when compared to sorted B220^{+} BM cells from WT control (Fig. 4B–D). These findings suggest that either Sca1-BCR-ABL^{p190} alone or *Pax5*-deficiency resulted in modest, but significant increases in glucose utilization and energy

Downloaded from http://aacrjournals.org/cancerres/article-pdf/78/10/2669/2764846/2669.pdf by guest on 05 February 2024

metabolism. Interestingly, while Sca1-BCR-ABL1^{P190} alone increased total ATP levels by ∼three-fold, deficiency in *Pax5* doubled the levels of total ATP (Sca1-BCR-ABL^{P190} pro-B cells carrying WT *Pax5*: ∼3-fold vs. Sca1-BCR-ABL^{P190}+Pax5$^{+/-}$ pro-B cells: ∼6-fold).

In addition, oxygen consumption rate (OCR) and ECAR were measured to monitor mitochondrial function (ATP turnover) and glycolytic profiles, respectively. Compared with *Pax5* WT pro-B cells, mitochondrial ATP production was increased by ∼1.4-fold in nonleukemic Sca1-BCR-ABL^{P190} pro-B cells. Interestingly, *Pax5*-deficiency resulted in additional increases in mitochondrial ATP production. In comparison to Pax5 WT pro-B cells, mitochondrial ATP production was increased by ∼2.3-fold in Sca1-BCR-ABL^{p190}+*Pax5*$^{+/-}$ pro-B cells (Fig. 4E). Glycolytic profiles were monitored under basal conditions (glycolytic activity) and in response to acute addition of oligomycin (an inhibitor of ATP synthase). Oligomycin suppresses mitochondrial ATP production, leading to increased compensatory glycolysis to meet the energy demands of the cell (glycolytic capacity). Consistent with the above observations, glycolytic activities of both nonleukemic Sca1-BCR-ABL^{P190} pro-B cells (∼2-fold) and Pax5-deficient pro-B cells (∼2- to 3-fold) were higher compared with WT pro-B cells (Fig. 4F). Furthermore, glycolytic capacities of Sca1-BCR-ABL^{P190} pro-B cells (∼2-fold) and Pax5-deficient pro-B cells (∼4- to 5-fold) were increased (Fig. 4G). Significant energy supply to fuel macromolecular synthesis for proliferation is required during transformation of leukemia cells. Recently, it has been demonstrated that PAX5 functions as a metabolic barrier through transcriptional repression of *GLUT*1/3/6 (glucose transporters), *HK*2/3, *PFKL*, *PGAM*, *PYG*L, and *G6PD* (glucose utilization) as PAX5 targets in pB-ALL (38). Here, we identified novel metabolic targets of PAX5 (*IDH1*, *G6PC3*, *GAPDH*, *PGK1*, *MYC*, *ENO1*, and *ACO1*) and observed a similar metabolic signature in human pB-ALLs. Furthermore, we demonstrated that *Pax5*-deficiency led to increased glucose utilization and energy metabolism, which is further enhanced in cells primed by the BCR-ABL^{P190} oncogene at the stage of HS/PCs.

Discussion

The common belief in pB-ALL development is that the disease originates from pro-B/pre-B cells that critically depend on survival signals (39–41). However, the *BCR-ABL^{p190}* oncogene is not able to confer self-renewal stem cell-like properties to progenitors in mice (42). In agreement with this view, both, twin-based data, and the high frequency of preleukemic clones carrying BCR-ABL^{P190} oncogenic lesions frequently found in neonatal cord blood, support that the *BCR-ABL^{p190}* gene fusion creates a preleukemic clone remaining clinically silent until secondary mutational events give rise to a full blown leukemia (1, 2). Common among these secondary events are alterations disrupting the *PAX5* gene, occurring in around one-third of pB-ALLs in general, and in almost every second case of the high-risk BCR-ABL-positive pB-ALL (27). Mostly, these mutations result in reduced Pax5 transcriptional activity, altering target gene expression (43), which highlights the fact that *PAX5* deletions might contribute to leukemogenesis (27). In this setting, and as opposed to its role as susceptible gene in infection-exposure-driven pB-ALL (22), *PAX5* deficiency seems to retain driver functions in established leukemia because it was previously shown that restoring endogenous *Pax5* expression can trigger disease remission in mice (18). However, the critical question of how BCR-ABL^{P190} and PAX5 loss contribute to pB-ALL leukemogenesis remained undefined. Here, we demonstrate that limited expression of the *BCR-ABL^{p190}* oncogene within HS/PCs is capable of inducing pB-ALL, further suggesting that BCR-ABL^{P190} favors the appearance of an aberrant precursor B-cell compartment in the BM. Significant reduction of Pax5 activity can be the critical factor in this experimental set up producing the selection pressure in favor of pB-ALL progression, because pB-ALL incidence drastically accelerated in Sca1-BCR-ABL^{P190}+*Pax5*$^{+/-}$ mice with the accumulation of additional somatic *Pax5* lesions in the remaining *Pax5* WT allele. The emergence of these inactivating Pax5 variants could further be linked to disease onset, because amplicon sequencing of PB mononuclear cells taken at routine intervals confirmed their absence prior to first phenotypic signs of illness. This observation highlights the fact that Pax5 loss does not function as a susceptibility event in BCR-ABL^{P190}-pB-ALL development. In our model, the *BCR-ABL^{p190}* oncogene primes HS/PCs for the acquisition of secondary *Pax5* mutations/deletions, which then act as the driving event in promoting clonal selection in pro-B/pre-B cells. Mechanistically, we show that the oncogenic capacity of reduced Pax5 transcriptional activity in the Sca1-BCR-ABL^{P190} Pax5 deficient preleukemic clone is the result of a specific metabolic reprogramming characterized by elevated levels of glucose utilization and energy metabolism. The metabolic reprogramming is further shown by increased glycolytic capacity. Augmented glycolytic capacity indicates that Sca1-BCR-ABL^{P190} Pax5-deficient ALL cells have an elevated ability to engage compensatory glycolysis to restore ATP levels when mitochondrial ATP production is inhibited. This metabolic rewiring is enhanced when Pax5 loss acts as a secondary event in the context of BCR-ABL^{P190} susceptibility and is an early event recapitulated in healthy Sca1-BCR-ABL^{P190} Pax5-deficient pro-B cells.

Transformation of leukemia cells imposes significant requirements for energy supply to support macromolecular synthesis for proliferation. Recent studies have identified *GLUT*1/3/6 (glucose transporters), *HK*2/3, *PFKL*, *PGAM*, *PYG*L, and *G6PD* (glucose utilization) as PAX5 targets in pB-ALL (38). Using our mouse models, we identified novel PAX5 targets that are involved in glucose utilization and energy metabolism (*IDH1*, *G6PC3*, *GAPDH*, *PGK1*, *MYC*, *ENO1*, and *ACO1*) and showed that deficiency in Pax5 resulted in metabolic reprogramming towards glucose utilization and energy metabolism. Importantly, gene expression analysis showed that human pB-ALLs carry a similar metabolic signature, illustrating that metabolic reprogramming could be a vulnerability and potential therapeutic target in the treatment of pB-ALLs.

IKZF1 (IKAROS) is known to be a hallmark of Ph^{+} (44), and Ph-like ALL (45) and similar to PAX5, IKZF1 was shown to act as a metabolic gatekeeper, preventing malignant transformation (38). Although, we were not able to identify inactivating mutations/deletions in the here presented model, we observed downregulation of Ikzf1 in the expression profiles of Sca1-BCR-ABL^{P190}+*Pax5*$^{+/-}$pB-ALLs. Therefore, it will be interesting to further assess the pB-ALL incidence, mutational landscape, and metabolic profile of Sca1-BCR-ABL^{P190}+*Ikzf1*$^{+/-}$ mice as depicted here for Pax5.

Taken together, our results show that Pax5 is rate-limiting for BCR-ABL^{P190} leukemogenesis. This supports a driver role for *Pax5* deficiency in a preleukemic cell by determining to a large extent

Downloaded from http://aacrjournals.org/cancerres/article-pdf/78/10/2669/2764846/2669.pdf by guest on 05 February 2024

the clonal evolution of BCR-ABL^{p190} pB-ALL development through metabolic reprogramming. Overall, the findings presented herein are important for encouraging novel interventions that might help to prevent conversion of BCR-ABL^{p190} preleukemic cells.

Disclosure of Potential Conflicts of Interest

No potential conflicts of interest were disclosed.

Authors' Contributions

Conception and design: A. Martín-Lorenzo, L.N. Chan, M. Müschen, I. Sánchez-García, A. Borkhardt, C. Vicente-Dueñas, J. Hauer

Development of methodology: A. Martín-Lorenzo, F. Auer, L.N. Chan, I. García-Ramírez, I. González-Herrero, G. Rodríguez-Hernández, A. Orfao, M. Müschen, I. Sánchez-García, C. Vicente-Dueñas, J. Hauer

Acquisition of data (provided animals, acquired and managed patients, provided facilities, etc.): A. Martín-Lorenzo, F. Auer, L.N. Chan, I. García-Ramírez, I. González-Herrero, G. Rodríguez-Hernández, M. Gombert, O. Blanco, M.B. García-Cenador, M. Müschen, I. Sánchez-García, C. Vicente-Dueñas

Analysis and interpretation of data (e.g., statistical analysis, biostatistics, computational analysis): A. Martín-Lorenzo, F. Auer, L.N. Chan, I. García-Ramírez, I. González-Herrero, G. Rodríguez-Hernández, C. Bartenhagen, M. Dugas, M. Gombert, S. Ginzel, D. Alonso-López, J. De Las Rivas, M.B. García-Cenador, M. Müschen, I. Sánchez-García, A. Borkhardt, J. Hauer

Writing, review, and/or revision of the manuscript: A. Martín-Lorenzo, F. Auer, L.N. Chan, I. González-Herrero, G. Rodríguez-Hernández, A. Orfao, M.B. García-Cenador, M. Müschen, I. Sánchez-García, A. Borkhardt, C. Vicente-Dueñas, J. Hauer

Administrative, technical, or material support (i.e., reporting or organizing data, constructing databases): A. Martín-Lorenzo, S. Ginzel, F.J. García-Criado,

Study supervision: M. Müschen, I. Sánchez-García, A. Borkhardt, C. Vicente-Dueñas

Acknowledgments

We are indebted to all members of our groups for useful discussions and for their critical reading of the manuscript. We are grateful to Dr. Meinrad Busslinger for the *Pax5*$^{+/-}$ mice and the *luc-CD19* construct. We thank Dr. Christophe Paillart at the Mouse Metabolism Core of the UCSF Diabetes Research Center (DRC) for help with metabolic assays using the XFe24 Flux Analyzer. J. Hauer has been supported by the German Cancer Aid (Project 110997 and Translational Oncology Program 70112951), the German Jose Carreras Foundation (DJCLS 02R/2016), the Kinderkrebsstiftung (2016/17), and the "Elterninitiative Kinderkrebstiftung e.V." S. Ginzel has been supported by a scholarship of the Hochschule Bonn-Rhein-Sieg. M. Müschen is an HHMI Faculty Scholar (HHMI-55108547) and supported by NIH/NCI through an Outstanding Investigator Award (R35CA197628, R01CA137060, R01CA157644, R01CA172558, R01CA213138) to M. Müschen, a Wellcome Trust Senior Investigator Award, the Leukemia and Lymphoma Society, the Norman and Sadie Lee Foundation (for Pediatric Cancer, to M. Müschen), and the Dr. Ralph and Marian Falk Medical Research Trust (to M. Müschen), Cancer Research Institute through a Clinic and Laboratory Integration Program grant (to M. Müschen) and the California Institute for Regenerative Medicine (CIRM) through DISC2-10061. A. Borkhardt has been supported by the German Children's Cancer Foundation and the Federal Ministry of Education and Research, Bonn, Germany. Research in I. Sánchez-García's group is partially supported by FEDER and by MINECO (SAF2012-32810, SAF2015-64420-R, and Red de Excelencia Consolider OncoBIO SAF2014-57791-REDC), Instituto de Salud Carlos III (PIE14/00066), ISCIII- Plan de Ayudas IBSAL 2015 Proyectos Integrados (IBY15/00003), by Junta de Castilla y León (BIO/SA51/15, CSI001U14, UIC-017, and CSI001U16), Fundacion Inocente Inocente and by the ARIMMORA project [European Union's Seventh Framework Programme (FP7/2007-2013) under grant agreement no. 282891]. I. Sánchez-García's lab is a member of the EuroSyStem and the DECIDE Network funded by the European Union under the FP7 program. A. Borkhardt and I. Sánchez-García have been supported by the German Carreras Foundation (DJCLS R13/26). Research in C. Vicente-Dueñas's group is partially supported by FEDER, Ministerio de Economía y Competitividad ("Miguel Servet" Grant - CP14/00082 - AES 2013-2016) and (PI17/00167) from the Instituto de Salud Carlos III. A. Martín-Lorenzo and G. Rodríguez-Hernández were supported by FSE-Conserjería de Educación de la Junta de Castilla y León (CSI001-13 and CSI001-15, respectively). F. Auer was supported by a Deutsche Forschungsgemeinschaft (DFG) fellowship (AU 525/1-1).

The costs of publication of this article were defrayed in part by the payment of page charges. This article must therefore be hereby marked *advertisement* in accordance with 18 U.S.C. Section 1734 solely to indicate this fact.

Received October 24, 2017; revised January 23, 2018; accepted February 23, 2018; published first February 28, 2018.

References

1. Cazzaniga G, van Delft FW, Lo Nigro L, Ford AM, Score J, Iacobucci I, et al. Developmental origins and impact of BCR-ABL1 fusion and IKZF1 deletions in monozygotic twins with Ph+ acute lymphoblastic leukemia. Blood 2011;118:5559–64.
2. Kosik P, Skorvaga M, Durdik M, Jakl L, Nikitina E, Markova E, et al. Low numbers of pre-leukemic fusion genes are frequently present in umbilical cord blood without affecting DNA damage response. Oncotarget 2017; 8:35824–34.
3. Bose S, Deininger M, Gora-Tybor J, Goldman JM, Melo JV. The presence of typical and atypical BCR-ABL fusion genes in leukocytes of normal individuals: biologic significance and implications for the assessment of minimal residual disease. Blood 1998;92:3362–7.
4. Duy C, Hurtz C, Shojaee S, Cerchietti L, Geng H, Swaminathan S, et al. BCL6 enables Ph+ acute lymphoblastic leukaemia cells to survive BCR-ABL1 kinase inhibition. Nature 2011;473:384–8.
5. Perez-Caro M, Gutierrez-Cianca N, Gonzalez-Herrero I, Lopez-Hernandez I, Flores T, Orfao A, et al. Sustained leukaemic phenotype after inactivation of BCR-ABLp190 in mice. Oncogene 2007;26:1702–13.
6. Heisterkamp N, Jenster G, ten Hoeve J, Zovich D, Pattengale PK, Groffen J. Acute leukaemia in bcr/abl transgenic mice. Nature 1990;344:251–3.
7. Castellanos A, Pintado B, Weruaga E, Arevalo R, Lopez A, Orfao A, et al. A BCR-ABL(p190) fusion gene made by homologous recombination causes B-cell acute lymphoblastic leukemias in chimeric mice with independence of the endogenous bcr product. Blood 1997;90: 2168–74.
8. Urbanek P, Wang ZQ, Fetka I, Wagner EF, Busslinger M. Complete block of early B cell differentiation and altered patterning of the posterior midbrain in mice lacking Pax5/BSAP. Cell 1994;79:901–12.
9. Miles C, Sanchez MJ, Sinclair A, Dzierzak E. Expression of the Ly-6E.1 (Sca-1) transgene in adult hematopoietic stem cells and the developing mouse embryo. Development 1997;124:537–47.
10. Perez-Caro M, Cobaleda C, Gonzalez-Herrero I, Vicente-Duenas C, Bermejo-Rodriguez C, Sanchez-Beato M, et al. Cancer induction by restriction of oncogene expression to the stem cell compartment. EMBO J 2009;28:8–20.
11. Edgar R, Domrachev M, Lash AE. Gene Expression Omnibus: NCBI gene expression and hybridization array data repository. Nucleic Acids Res 2002;30:207–10.
12. Subramanian A, Tamayo P, Mootha VK, Mukherjee S, Ebert BL, Gillette MA, et al. Gene set enrichment analysis: a knowledge-based approach for interpreting genome-wide expression profiles. Proc Nat Acad Sci USA 2005;102:15545–50.
13. Chiaretti S, Li X, Gentleman R, Vitale A, Wang KS, Mandelli F, et al. Gene expression profiles of B-lineage adult acute lymphocytic leukemia reveal genetic patterns that identify lineage derivation and distinct mechanisms of transformation. Clin Cancer Res 2005;11:7209–19.
14. Kohlmann A, Schoch C, Schnittger S, Dugas M, Hiddemann W, Kern W, et al. Pediatric acute lymphoblastic leukemia (ALL) gene expression signatures classify an independent cohort of adult ALL patients. Leukemia 2004;18:63–71.

Downloaded from http://aacrjournals.org/cancerres/article-pdf/78/10/2669/2764846/2669.pdf by guest on 05 February 2024

15. Green MR, Monti S, Dalla-Favera R, Pasqualucci L, Walsh NC, Schmidt-Supprian M, et al. Signatures of murine B-cell development implicate Yy1 as a regulator of the germinal center-specific program. Proc Nat Acad Sci USA 2011;108:2873–8.
16. Hakansson P, Nilsson B, Andersson A, Lassen C, Gullberg U, Fioretos T. Gene expression analysis of BCR/ABL1-dependent transcriptional response reveals enrichment for genes involved in negative feedback regulation. Gen Chrom Cancer 2008;47:267–75.
17. Delogu A, Schebesta A, Sun Q, Aschenbrenner K, Perlot T, Busslinger M. Gene repression by Pax5 in B cells is essential for blood cell homeostasis and is reversed in plasma cells. Immunity 2006;24:269–81.
18. Liu GJ, Cimmino L, Jude JG, Hu Y, Witkowski MT, McKenzie MD, et al. Pax5 loss imposes a reversible differentiation block in B-progenitor acute lymphoblastic leukemia. Genes Dev 2014;28:1337–50.
19. Revilla IDR, Bilic I, Vilagos B, Tagoh H, Ebert A, Tamir IM, et al. The B-cell identity factor Pax5 regulates distinct transcriptional programmes in early and late B lymphopoiesis. EMBO J 2012;31:3130–46.
20. Schebesta A, McManus S, Salvagiotto G, Delogu A, Busslinger GA, Busslinger M. Transcription factor Pax5 activates the chromatin of key genes involved in B cell signaling, adhesion, migration, and immune function. Immunity 2007;27:49–63.
21. Pfisterer U, Kirkeby A, Torper O, Wood J, Nelander J, Dufour A, et al. Direct conversion of human fibroblasts to dopaminergic neurons. Proc Nat Acad Sci USA 2011;108:10343–8.
22. Martin-Lorenzo A, Hauer J, Vicente-Duenas C, Auer F, Gonzalez-Herrero I, Garcia-Ramirez I, et al. Infection exposure is a causal factor in B-precursor acute lymphoblastic leukemia as a result of Pax5 inherited susceptibility. Cancer Discov 2015;5:1328–43.
23. Czerny T, Busslinger M. DNA-binding and transactivation properties of Pax-6: three amino acids in the paired domain are responsible for the different sequence recognition of Pax-6 and BSAP (Pax-5). Mol Cell Biol 1995;15:2858–71.
24. Sanchez-Garcia I, Grutz G. Tumorigenic activity of the BCR-ABL oncogenes is mediated by BCL2. Proc Nat Acad Sci USA 1995;92:5287–91.
25. Okabe M, Matsushima S, Morioka M, Kobayashi M, Abe S, Sakurada K, et al. Establishment and characterization of a cell line, TOM-1, derived from a patient with Philadelphia chromosome-positive acute lymphocytic leukemia. Blood 1987;69:990–8.
26. Vicente-Duenas C, Romero-Camarero I, Cobaleda C, Sanchez-Garcia I. Function of oncogenes in cancer development: a changing paradigm. EMBO J 2013;32:1502–13.
27. Mullighan CG, Goorha S, Radtke I, Miller CB, Coustan-Smith E, Dalton JD, et al. Genome-wide analysis of genetic alterations in acute lymphoblastic leukaemia. Nature 2007;446:758–64.
28. Shah S, Schrader KA, Waanders E, Timms AE, Vijai J, Miething C, et al. A recurrent germline PAX5 mutation confers susceptibility to pre-B cell acute lymphoblastic leukemia. Nat Genet 2013;45:1226–31.
29. van Zelm MC, van der Burg M, de Ridder D, Barendregt BH, de Haas EF, Reinders MJ, et al. Ig gene rearrangement steps are initiated in early human precursor B cell subsets and correlate with specific transcription factor expression. J Immunol 2005;175:5912–22.
30. Ross ME, Zhou X, Song G, Shurtleff SA, Girtman K, Williams WK, et al. Classification of pediatric acute lymphoblastic leukemia by gene expression profiling. Blood 2003;102:2951–9.
31. Robey RB, Hay N. Mitochondrial hexokinases, novel mediators of the antiapoptotic effects of growth factors and Akt. Oncogene 2006;25:4683–96.
32. Federzoni EA, Humbert M, Torbett BE, Behre G, Fey MF, Tschan MP. CEBPA-dependent HK3 and KLF5 expression in primary AML and during AML differentiation. Sci Rep 2014;4:4261.
33. Shestov AA, Liu X, Ser Z, Cluntun AA, Hung YP, Huang L, et al. Quantitative determinants of aerobic glycolysis identify flux through the enzyme GAPDH as a limiting step. eLife 2014;3:e03342.
34. Jun HS, Lee YM, Cheung YY, McDermott DH, Murphy PM, De Ravin SS, et al. Lack of glucose recycling between endoplasmic reticulum and cytoplasm underlies cellular dysfunction in glucose-6-phosphatase-beta-deficient neutrophils in a congenital neutropenia syndrome. Blood 2010;116:2783–92.
35. Akram M. Citric acid cycle and role of its intermediates in metabolism. Cell Biochem Biophys 2014;68:475–8.
36. Stine ZE, Walton ZE, Altman BJ, Hsieh AL, Dang CV. MYC, Metabolism, and Cancer. Cancer Discov 2015;5:1024–39.
37. Eberhard D, Jimenez G, Heavey B, Busslinger M. Transcriptional repression by Pax5 (BSAP) through interaction with corepressors of the Groucho family. EMBO J 2000;19:2292–303.
38. Chan LN, Chen Z, Braas D, Lee JW, Xiao G, Geng H, et al. Metabolic gatekeeper function of B-lymphoid transcription factors. Nature 2017;542:479–83.
39. Daley GQ, Van Etten RA, Baltimore D. Induction of chronic myelogenous leukemia in mice by the P210bcr/abl gene of the Philadelphia chromosome. Science 1990;247:824–30.
40. McLaughlin J, Chianese E, Witte ON. In vitro transformation of immature hematopoietic cells by the P210 BCR/ABL oncogene product of the Philadelphia chromosome. Proc Nat Acad Sci USA 1987;84:6558–62.
41. Muschen M. Rationale for targeting the pre-B-cell receptor signaling pathway in acute lymphoblastic leukemia. Blood 2015;125:3688–93.
42. Huntly BJ, Shigematsu H, Deguchi K, Lee BH, Mizuno S, Duclos N, et al. MOZ-TIF2, but not BCR-ABL, confers properties of leukemic stem cells to committed murine hematopoietic progenitors. Cancer cell 2004;6:587–96.
43. An Q, Wright SL, Konn ZJ, Matheson E, Minto L, Moorman AV, et al. Variable breakpoints target PAX5 in patients with dicentric chromosomes: a model for the basis of unbalanced translocations in cancer. Proc Nat Acad Sci USA 2008;105:17050–4.
44. Mullighan CG, Miller CB, Radtke I, Phillips LA, Dalton J, Ma J, et al. BCR-ABL1 lymphoblastic leukaemia is characterized by the deletion of Ikaros. Nature 2008;453:110–4.
45. Pui CH, Roberts KG, Yang JJ, Mullighan CG. Philadelphia chromosome-like acute lymphoblastic leukemia. Clin Lymph Myeloma Leukemia 2017;17:464–70.

Downloaded from http://aacrjournals.org/cancerres/article-pdf/78/10/2669/2764846/2669.pdf by guest on 05 February 2024